

¹ eo-tides: Tide modelling tools for large-scale satellite Earth observation analysis

³ **Robbi Bishop-Taylor**  ¹¶, **Claire Phillips**  ¹, **Stephen Sagar**  ¹, **Vanessa Newey**¹, and **Tyler Sutterley**  ²

⁵ 1 Geoscience Australia, Australia  ² University of Washington Applied Physics Laboratory, United States of America  ¶ Corresponding author

DOI: [10.xxxxxx/draft](https://doi.org/10.xxxxxx/draft)

Software

- [Review](#) ↗
- [Repository](#) ↗
- [Archive](#) ↗

Editor: [Open Journals](#) ↗

Reviewers:

- [@openjournals](#)

Submitted: 01 January 1970

Published: unpublished

License

Authors of papers retain copyright and release the work under a Creative Commons Attribution 4.0 International License ([CC BY 4.0](#)).

Summary

The eo-tides package provides powerful parallelized tools for integrating satellite Earth observation (EO) data with ocean tide modelling. The package provides a flexible Python-based toolkit for modelling and attributing tide heights to a time-series of satellite images based on the spatial extent and acquisition time of each satellite observation (Figure 1).

eo-tides leverages advanced tide modelling functionality from the pyTMD tide prediction software ([Sutterley et al., 2017](#)), combining this fundamental tide modelling capability with EO spatial analysis tools from odc-geo ([odc-geo contributors, 2024](#)). This allows tides to be modelled in parallel automatically using over 50 supported tide models, and returned in standardised pandas ([McKinney, 2010](#); [pandas development team, 2020](#)) and xarray ([Hoyer & Joseph, 2017](#)) data formats for further analysis.

Tools from eo-tides are designed to be applied directly to petabytes of freely available satellite data loaded from the cloud using Open Data Cube's odc-stac or datacube packages (e.g. using [Digital Earth Australia](#) or [Microsoft Planetary Computer's SpatioTemporal Asset Catalogues](#)). Additional functionality enables evaluating potential satellite-tide biases, and validating modelled tides using external tide gauge data — both important considerations for assessing the reliability and accuracy of coastal EO workflows. In combination, these open source tools support the efficient, scalable and robust analysis of coastal EO data for any time period or location globally.

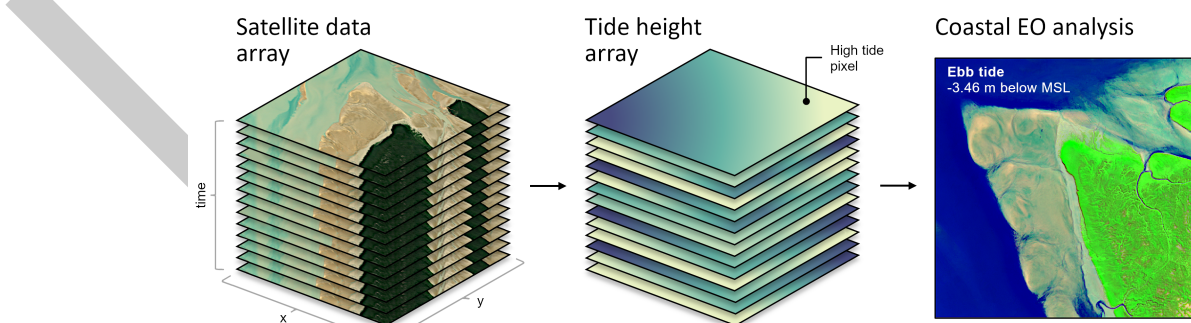


Figure 1: An example of a typical eo-tides coastal EO workflow, with tide heights being modelled into every pixel in a spatio-temporal stack of satellite data (for example, from ESA's Sentinel-2 or NASA/USGS Landsat), then combined to derive insights into dynamic coastal environments.

26 Statement of need

27 Satellite remote sensing offers an unparalleled method to view and examine dynamic coastal
28 environments over large temporal and spatial scales (Turner et al., 2021; Vitousek et al.,
29 2023). However, the variable and sometimes extreme influence of ocean tides in these regions
30 can complicate analyses, making it difficult to separate the influence of changing tides from
31 patterns of true coastal change over time (Vos et al., 2019). This is a particularly significant
32 challenge for continental- to global-scale coastal EO analyses, where failing to account for
33 complex tide dynamics can lead to inaccurate or misleading insights into coastal processes
34 observed by satellites.

35 Conversely, information about ocean tides can also provide unique environmental insights that
36 can greatly enhance the utility of coastal EO data. Conventionally, satellite data dimensions
37 consider the geographical “where” and the temporal “when” of data acquisition. The addition
38 of tide height as a new analysis dimension allows data to be filtered, sorted and analysed with
39 respect to tidal processes, delivering a powerful re-imagining of traditional multi-temporal EO
40 data analysis (Sagar et al., 2017). For example, satellite data can be analysed to focus on
41 specific ecologically-significant tidal stages (e.g. high, low tide, spring or neap tides) or on
42 particular tidal processes (e.g. ebb or flow tides; Sent et al. (2025)).

43 This concept has been used to map tidally-corrected annual coastlines from Landsat satellite
44 data at continental scale (Bishop-Taylor et al., 2021), generate maps of the extent and elevation
45 of the intertidal zone (Bishop-Taylor et al., 2019; Murray et al., 2012; Sagar et al., 2017), and
46 create tidally-constrained imagery composites of the coastline at low and high tide (Sagar et
47 al., 2018). However, these approaches have been historically based on bespoke, closed-source
48 or difficult to install tide modelling tools, limiting the reproducibility and portability of these
49 techniques to new coastal EO applications. To support the next generation of coastal EO
50 workflows, there is a pressing need for new open-source approaches for combining satellite data
51 with tide modelling.

52 The `eo-tides` package aims to address these challenges by providing a set of performant
53 open-source Python tools for attributing satellite EO data with modelled ocean tides. This
54 functionality is provided in five main analysis modules (`utils`, `model`, `eo`, `stats`, `validation`)
55 which are described briefly below.

56 Key functionality

57 Setting up tide models

58 A key barrier to utilising tide modelling in EO workflows is the complexity and difficulty of
59 initially setting up global ocean tide models for analysis. To address this, the `eo_tides.utils`
60 module contains useful tools for preparing tide model data files for use in `eo-tides`. This
61 includes the `list_models` function that provides visual feedback on the tide models a user has
62 available in their system, while highlighting the naming conventions and directory structures
63 required by the underlying pyTMD tide prediction software (Figure 2).

64 Running tide modelling using the default tide modelling data provided by external providers can
65 be slow due to the large size of these files — especially for recent high-resolution models like
66 FES2022 (Carrere et al., 2022). To improve tide modelling performance, it can be extremely
67 useful to clip tide model files to a smaller region of interest (e.g. the extent of a country
68 or coastal region). The `clip_models` function can be used to automatically clip all suitable
69 NetCDF-format model data files to a user-supplied bounding box, potentially improving tide
70 modelling performance by over an order of magnitude.

71 These tools are accompanied by comprehensive documentation explaining how to set up several
72 of the most commonly used global ocean tide models, including details on how to download or
73 request access to model files, and how to uncompress and arrange the data on disk.

	Model	Expected path
	EOT20	tide_models/EOT20/ocean_tides
	FES2014	tide_models/fes2014/ocean_tide
	HAMTIDE11	tide_models/hamtide
	TPXO9.1	tide_models/TPXO9.1/DATA
...

Summary:
Available models: 2/50

Figure 2: An example output from `list_tides`, providing a useful summary table which clearly identifies available and supported tide models.

74 Modelling tides

75 The `eo_tides.model` module is powered by advanced tide modelling functionality from the
 76 pyTMD Python package ([Sutterley et al., 2017](#)).

77 pyTMD is an open-source tidal prediction software that aims to simplify the calculation of ocean
 78 and earth tides. Tides are frequently decomposed into harmonic constants (or constituents)
 79 associated with the relative positions of the sun, moon and Earth. For ocean tides, pyTMD.io
 80 contains routines for reading major constituent values from commonly available tide models,
 81 and interpolating those values to spatial locations. Information for each of the supported tide
 82 models is stored within a JSON database that is supplied with pyTMD. pyTMD.astro contains
 83 routines for computing the positions of celestial bodies for a given time. Namely for ocean
 84 tides, pyTMD computes the longitudes of the sun (S), moon (H), lunar perigee (P), ascending
 85 lunar node (N) and solar perigee (PP). pyTMD.arguments contains routines for combining the
 86 astronomical coefficients with the “Doodson number” of each constituent, along with routines
 87 for adjusting the amplitude and phase of each constituent based on their modulations over the
 88 18.6 year nodal period. Finally, pyTMD.predict uses results from those underlying functions to
 89 predict tidal values at a given location and time.

90 To support integration with satellite EO data, the `model_tides` function from `eo_tides.model`
 91 wraps pyTMD functionality to return predicted tides in a standardised `pandas.DataFrame` format
 92 containing information about the tide model, location and time period of each modelled tide.
 93 This allows large analyses to be broken into smaller discrete chunks that can be processed in
 94 parallel before being combined as a final step. Parallelisation in `eo-tides` is automatically
 95 optimised based on the number of available workers and the number of requested tide models
 96 and tide modelling locations. This built-in parallelisation can significantly improve tide modelling
 97 performance, especially when run on a large multi-core machine ([Table 1](#)).

Table 1: A benchmark comparison of tide modelling performance with parallelisation on vs. off. This comparison was performed on an 8-core and 32-core Linux machine, for a typical large-scale analysis involving a month of hourly tides modelled at 10,000 modelling locations using three tide models (FES2022, TPXO10, GOT5.6).

Cores	Parallelisation	No parallelisation	Speedup
8	2min 46s ± 663 ms	9min 28s ± 536 ms	3.4x
32	55.9 s ± 560 ms	9min 24s ± 749 ms	10.1x

98 The `model_tides` function is primarily intended to support more complex EO-related tide
 99 modelling functionality in the downstream `eo_tides.eo` module. However it can also be
 100 used independently of EO data, for example for any application that requires a time series
 101 of modelled tide heights. In addition to modelling tide heights, the `model_phases` function
 102 can also be used to calculate the phase of the tide at any location and time. This can be
 103 used to classify tides into high and low tide observations, or determine whether the tide was
 104 rising (i.e. flow tide) or falling (i.e. ebb tide) — information that can be critical for correctly
 105 interpreting satellite-observed coastal processes like changing turbidity and ocean colour (Sent
 106 et al., 2025).

107 Combining tides with satellite data

108 The `eo_tides.eo` module contains the package's core functionality, focusing on tools for
 109 attributing satellite data with modelled tide heights. These tools can be applied to xarray-
 110 format satellite data from any coastal location on the planet, for example using data loaded
 111 from the cloud using the [Open Data Cube](#) and SpatioTemporal Asset Catalogue ([STAC](#)
 112 [contributors, 2024](#)).

113 For tide attribution, eo-tides offers two approaches that differ in complexity and performance:
 114 `tag_tides` and `pixel_tides` ([Table 2](#)). The `tag_tides` function provides a fast and efficient
 115 method for small scale applications where tides are unlikely to vary across a study area. This
 116 approach allocates a single tide height to each satellite data timestep, based on the geographic-
 117 centroid of the dataset and the acquisition time of each image. Having tide height as a variable
 118 allows the selection and analysis of satellite data based on tides. For example, all available
 119 satellite observations for an area of interest could be sorted by tide height, or used to extract
 120 and compare the lowest and highest tide images in the time series.

121 Tide however typically exhibit spatial variability, with sea levels sometimes varying by up to
 122 metres in height across short distances in regions of complex and extreme tidal dynamics. This
 123 means that a single satellite image may often capture a range of contrasting tide conditions,
 124 making a single modelled tide per image an over-simplification of reality. For larger scale coastal
 125 EO analysis, the `pixel_tides` function can be used to seamlessly model tides through both
 126 time and space, producing a three-dimensional "tide height" datacube that can be integrated
 127 with satellite data. For efficient processing, `pixel_tides` 'models tides into a customisable
 128 low resolution grid surrounding each satellite image in the time series. These modelled tides
 129 are then re-projected back into the original resolution of the input satellite image, returning a
 130 unique tide height for every individual satellite pixel through time ([Figure 3](#)).

Table 2: Comparison of the `tag_tides` and `pixel_tides` functions.

<code>tag_tides</code>	<code>pixel_tides</code>
<ul style="list-style-type: none"> - Assigns a single tide height to each timestep/satellite image - Ideal for local or site-scale analysis - Fast, low memory use - Single tide height per image can produce artefacts in complex tidal regions 	<ul style="list-style-type: none"> - Assigns a tide height to every individual pixel through time to capture spatial tide dynamics - Ideal for regional to global-scale coastal product generation - Slower, higher memory use - Produce spatially seamless results across large extents by applying analyses at the pixel level

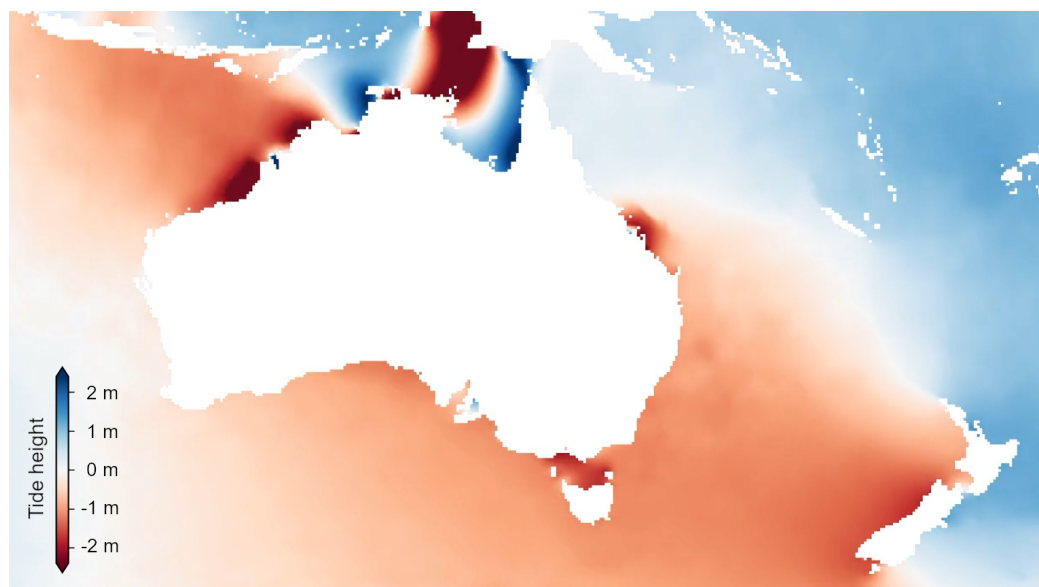


Figure 3: An example tide height output produced by the `pixel_tides` function, showing spatial variability in tides across Australasia for a single timestep.

131 **Calculating tide statistics and satellite biases**

132 The `eo_tides.stats` module contains tools for calculating statistics describing local tide
 133 dynamics, as well as biases caused by interactions between tidal processes and satellite orbits.
 134 Complex tide aliasing interactions between temporal tide dynamics and the regular overpass
 135 timing of sun-synchronous satellite sensors can prevent these satellites from observing the
 136 entire tidal cycle (Eleveld et al., 2014; Sent et al., 2025). Biases in satellite coverage of the
 137 tidal cycle can mean that tidal extremes (e.g. the lowest or highest tides at a location) or
 138 particular tidal processes may either never be captured by satellites, or be over-represented in
 139 the satellite record. Local tide dynamics can cause these biases to vary greatly both through
 140 time and space, making it challenging to compare coastal processes consistently across large
 141 spatial extents using EO data (Bishop-Taylor et al., 2019).

142 To ensure that coastal EO analyses are not inadvertently affected by tide biases, it is important
 143 to understand how well tides observed by satellites capture the full astronomical tide range at
 144 a location. The `tide_stats` function compares the subset of tides observed by satellite data
 145 against the full range of tides modelled at a regular interval through time across the entire
 146 time period covered by the satellite dataset. This comparison is used to calculate several useful
 147 statistics that summarise how well a satellite time series captures real-world tidal conditions
 148 (Bishop-Taylor et al., 2019). These statistics include:

- 149 1. Spread: The proportion of the modelled astronomical tidal range that was observed by
 150 satellites. A high value indicates good coverage of the tide range.
- 151 2. High-tide offset: The proportion of the highest tides never observed by satellites, relative
 152 to the modelled astronomical tidal range. A high value indicates that the satellite data
 153 never captures high tides.
- 154 3. Low-tide offset: The proportion of the lowest tides never observed by satellites, relative
 155 to the modelled astronomical tidal range. A high value indicates that the satellite data
 156 never captures low tides.

157 A satellite tide bias investigation for a coastal area of interest will return an automated report
 158 and plot (Figure 4), adding insightful tide-based context to a coastal EO analysis:

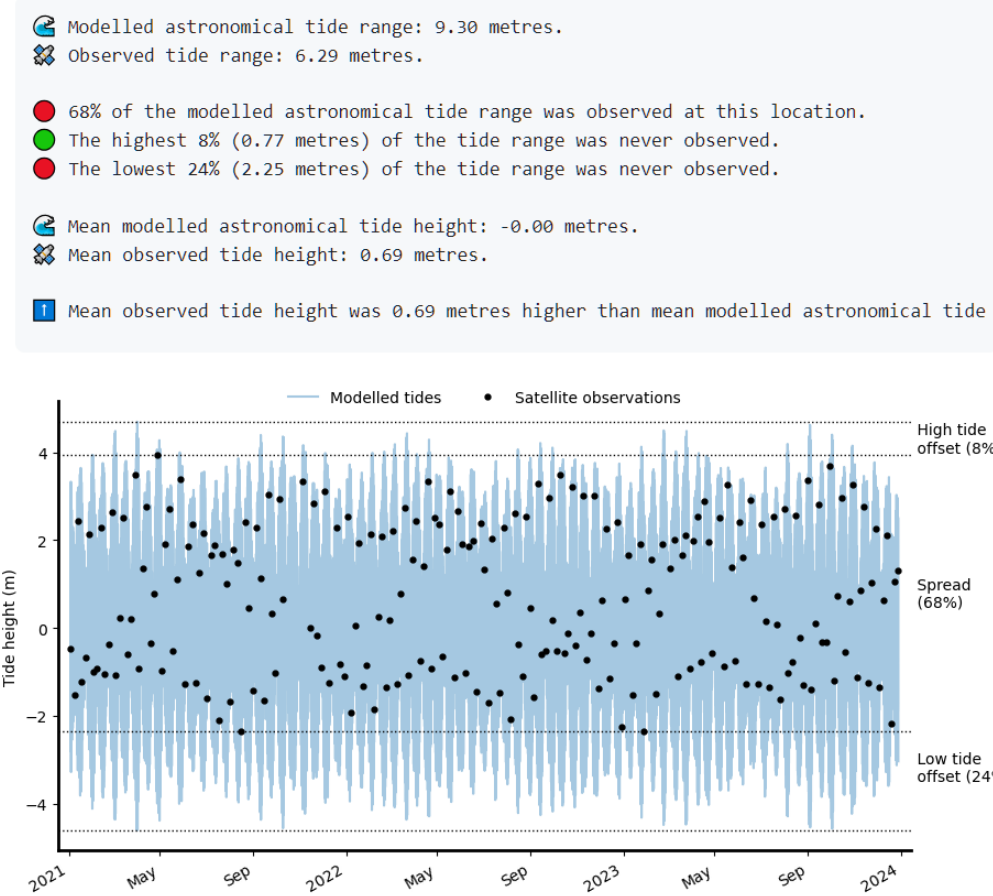


Figure 4: In this example satellite time series, the data captured a biased proportion of the tide range: only observing ~68% of the modelled astronomical tide range, and never observing the lowest 24% of tides. The plot visually demonstrates the relationships between satellite observed tide heights (black dots) and modelled astronomical tide height (blue lines) at this location.

159 Validating modelled tide heights

160 The `eo_tides.validation` module contains tools for validating modelled tides against observed
 161 sea level data. The tide models supported by `eo-tides` can vary significantly in accuracy
 162 across the world's coastlines. Evaluating the accuracy of modelled tides is critical for ensuring
 163 that resulting marine or coastal EO analyses are reliable and useful.

164 Validation functionality in `eo-tides` provides a convenient tool for loading high-quality sea-level
 165 measurements from the GESLA Global Extreme Sea Level Analysis (Haigh et al., 2023) archive
 166 – a global dataset of almost 90,713 years of sea level data from 5,119 records across the world.
 167 The `load_gauge_gesla` function allows GESLA data to be loaded for the same location and
 168 time period as a satellite time series. Differences between modelled and observed tide heights
 169 can then be quantified through the calculation of accuracy statistics that include the Root
 170 Mean Square Error (RMSE), Mean Absolute Error (MAE), R-squared and bias ([Figure 5](#)).

171 Furthermore, different ocean tide models perform differently in different coastal locations.
 172 `eo-tides` allows multiple tide models to be compared against GESLA data simultaneously
 173 ([Figure 5](#)), empowering users to make informed decisions and choose the optimal tide models
 174 for their specific location or application.



Figure 5: An example comparison of modelled tides from multiple global ocean tide models (EOT20, GOT5.5, HAMTIDE11) against observed sea level data from the Broome 62650 GESLA tide gauge, Western Australia.

175 Research projects

176 Early versions of functions provided in `eo-tides` has been used for continental-scale modelling
 177 of the elevation and exposure of Australia's intertidal zone ([Bishop-Taylor et al., 2024](#)), multi-
 178 decadal shoreline mapping across Australia ([Bishop-Taylor et al., 2021](#)) and [Africa](#), and to
 179 support tide correction for satellite-derived shorelines as part of the `CoastSeg` Python package
 180 ([Fitzpatrick et al., 2024](#)).

181 Acknowledgements

182 Functions from `eo-tides` were originally developed in the Digital Earth Australia Notebooks
 183 and Tools repository ([Krause et al., 2021](#)). The authors would like to thank all DEA Notebooks
 184 contributors and maintainers for their invaluable assistance with code review, feature suggestions
 185 and code edits. This paper is published with the permission of the Chief Executive Officer,
 186 Geoscience Australia. Copyright Geoscience Australia (2025).

187 References

- 188 Bishop-Taylor, R., Nanson, R., Sagar, S., & Lymburner, L. (2021). Mapping Australia's
 189 Dynamic Coastline at Mean Sea Level using Three Decades of Landsat Imagery. *Remote
 190 Sensing of Environment*, 267, 112734. <https://doi.org/10.1016/j.rse.2021.112734>
- 191 Bishop-Taylor, R., Phillips, C., Newey, V., & Sagar, S. (2024). *Digital Earth Australia Intertidal*.
 192 Commonwealth of Australia (Geoscience Australia). <https://doi.org/10.26186/149403>
- 193 Bishop-Taylor, R., Sagar, S., Lymburner, L., & Beaman, R. J. (2019). Between the tides:
 194 Modelling the elevation of australia's exposed intertidal zone at continental scale. *Estuarine,
 195 Coastal and Shelf Science*, 223, 115–128. <https://doi.org/10.1016/j.ecss.2019.03.006>
- 196 Carrere, L., Lyard, F., Cancet, M., Allain, D., Dabat, M.-L., Fouchet, E., Sahuc, E., Faugere,
 197 Y., Dibarboire, G., & Picot, N. (2022). A new barotropic tide model for global ocean:
 198 FES2022. *2022 Ocean Surface Topography Science Team Meeting*, 43.
- 199 Eleveld, M. A., Van der Wal, D., & Van Kessel, T. (2014). Estuarine suspended partic-
 200 uulate matter concentrations from sun-synchronous satellite remote sensing: Tidal and
 201 meteorological effects and biases. *Remote Sensing of Environment*, 143, 204–215.
- 202 Fitzpatrick, S., Buscombe, D., Warrick, J. A., Lundine, M. A., & Vos, K. (2024). *CoastSeg*: An
 203 accessible and extendable hub for satellite-derived-shoreline (SDS) detection and mapping.

- 204 *Journal of Open Source Software*, 9(99), 6683. <https://doi.org/10.21105/joss.06683>
- 205 Haigh, I. D., Marcos, M., Talke, S. A., Woodworth, P. L., Hunter, J. R., Hague, B. S.,
206 Arns, A., Bradshaw, E., & Thompson, P. (2023). GESLA version 3: A major update to
207 the global higher-frequency sea-level dataset. *Geoscience Data Journal*, 10(3), 293–314.
208 <https://doi.org/https://doi.org/10.1002/gdj3.174>
- 209 Hoyer, S., & Joseph, H. (2017). xarray: N-d labeled arrays and datasets in python. *Journal of*
210 *Open Research Software*, 5(1). <https://doi.org/10.5334/jors.148>
- 211 Krause, C., Dunn, B., Bishop-Taylor, R., Adams, C., Burton, C., Alger, M., Chua, S., Phillips, C.,
212 Newey, V., Kouzoubov, K., Leith, A., Ayers, D., & Hicks, A. (2021). *Digital Earth Australia*
213 *notebooks and tools repository*. <https://github.com/GeoscienceAustralia/dea-notebooks/>;
214 Commonwealth of Australia (Geoscience Australia). <https://doi.org/10.26186/145234>
- 215 McKinney, Wes. (2010). Data Structures for Statistical Computing in Python. In Stéfan van
216 der Walt & Jarrod Millman (Eds.), *Proceedings of the 9th Python in Science Conference*
217 (pp. 56–61). <https://doi.org/10.25080/Majora-92bf1922-00a>
- 218 Murray, N. J., Phinn, S. R., Clemens, R. S., Roelfsema, C. M., & Fuller, R. A. (2012).
219 Continental scale mapping of tidal flats across east asia using the landsat archive. *Remote*
220 *Sensing*, 4(11), 3417–3426.
- 221 odc-geo contributors. (2024). Opendatacube/odc-geo. In *Github repository*. GitHub.
222 <https://github.com/opendatacube/odc-geo>
- 223 pandas development team. (2020). *Pandas-dev/pandas: pandas* (latest). Zenodo. <https://doi.org/10.5281/zenodo.3509134>
- 225 Sagar, S., Phillips, C., Bala, B., Roberts, D., Lymburner, L., & Beaman, R. J. (2018).
226 Generating continental scale pixel-based surface reflectance composites in coastal regions
227 with the use of a multi-resolution tidal model. *Remote Sensing*, 10(3), 480. <https://doi.org/10.3390/rs10030480>
- 229 Sagar, S., Roberts, D., Bala, B., & Lymburner, L. (2017). Extracting the intertidal extent and
230 topography of the australian coastline from a 28 year time series of landsat observations.
231 *Remote Sensing of Environment*, 195, 153–169.
- 232 Sent, G., Antunes, C., Spyракος, E., Jackson, T., Atwood, E. C., & Brito, A. C. (2025). What
233 time is the tide? The importance of tides for ocean colour applications to estuaries. *Remote*
234 *Sensing Applications: Society and Environment*, 37, 101425.
- 235 STAC contributors. (2024). *SpatioTemporal Asset Catalog (STAC) specification*. <https://stacspec.org>
- 237 Sutterley, T. C., Alley, K., Brunt, K., Howard, S., Padman, L., & Siegried, M. (2017). *pyTMD:*
238 *Python-based tidal prediction software*. Zenodo. <https://doi.org/10.5281/zenodo.5555395>
- 239 Turner, I. L., Harley, M. D., Almar, R., & Bergsma, E. W. J. (2021). Satellite optical imagery
240 in Coastal Engineering. *Coastal Engineering*, 167, 103919. <https://doi.org/10.1016/j.coastaleng.2021.103919>
- 242 Vitousek, S., Buscombe, D., Vos, K., Barnard, P. L., Ritchie, A. C., & Warrick, J. A. (2023).
243 The future of coastal monitoring through satellite remote sensing. *Cambridge Prisms:*
244 *Coastal Futures*, 1, e10. <https://doi.org/10.1017/cft.2022.4>
- 245 Vos, K., Splinter, K. D., Harley, M. D., Simmons, J. A., & Turner, I. L. (2019). CoastSat: A
246 Google Earth Engine-enabled Python toolkit to extract shorelines from publicly available
247 satellite imagery. *Environmental Modelling & Software*, 122, 104528. <https://doi.org/10.1016/j.envsoft.2019.104528>